http://marte2.sid.inpe.br/rep/sid.inpe.br/marte2/2019/09.04.18.27

COMBINATION OF SPECTRAL INDICES FOR BURNED AREA DETECTION IN THE BRAZILIAN AMAZONIA

Mikhaela Aloísia Jéssie Santos Pletsch[1], Thales Vaz Penha[1], Celso Henrique Leite Silva Junior[1], Thales Sehn Körting[1], Luiz Eduardo Oliveira e Cruz de Aragão[1], Liana Oighenstein Anderson[2], and Fabiano Morelli[1]

[1]Instituto Nacional de Pesquisas Espaciais - INPE. Av. dos Astronautas, 1.758 - Jardim da Granja, São José dos Campos - SP, Brasil, 12227-010. E-mail: mikhaela.pletsch; thales.penha; celso.junior; thales.korting; luiz.aragao; fabiano.morelli@inpe.br; [2]Centro Nacional de Monitoramento e Alertas de Desastres Naturais - CEMADEN. Estrada Doutor Altino Bondensan, 500 - Parque Tecnológico de São José dos Campos, São José dos Campos - SP, Brasil, 12247-016. E-mail: liana.anderson@cemaden.gov.br

ABSTRACT

Spectral Indices (SI) are widely used for remote sensing application because they enhance targeted features in optical images through the algebraic combination of spectral bands. There is a large variety of SI, in which the performance varies depending on the user's application. Considering the different emphases that spectral indices may offer, here we present a test-case based on the combination of 10 SI in a three channels remote sensing image (Red; Green; Blue - RGB) aiming to highlight burned areas from other targets such as vegetation and water. This process generated 120 possible combinations without repetition. With spatial resolution of 30m, the proposed method was able to achieve an accuracy between 0,21 and 0.86, according to Cohen's Kappa coefficient. The two groups of indices MIRBI, NBR2, EVI, MNDWI and CSI; and BAI, NBR and NDVI were the most inaccurate and accurate indices, respectively, identified for the study site.

Key words — Rainforest, Landsat-8, Spectral Index, Forest Fires, Burnt Area.

1. INTRODUCTION

Fire is one of the main threats faced by Amazonia, the largest rainforest worldwide [1]. Although detecting Burned Areas (BA) is essential in order to monitoring fire risks, impacts and management, generating accurate BA products for Amazonia is difficult due to different factors, such as cloud coverage, presence of cloud shadows, forest seasonality, variability and temporal development of the spectral characteristics of the BA, imagery temporal resolution and products accuracy [2, 3, 4]. Among the available remote sensing approaches for BA detection, the MCD64A1 product from MODIS sensor [5] presents daily to two-days temporal resolution. However, its spatial resolution of 500m is not suitable for fine-scale analysis of the spatial extent of BA. Therefore, for such application a higher spatial resolution data would be recommended, for instance at medium spatial resolution [3], which ranges from 10 to 50m [6].

Within the context of medium resolution data, different authors reported the importance of the Linear Spectral Mixture Model (LSMM), which can be applied in any spatial resolution data [7], [8]. The LSMM considers that the value of a pixel in an image represents the linear mixture of the different elements in the pixel. As such, the model is related to the spectral response of pure pixels, called *endmembers* [9]. The LSMM is commonly applied using as input surface reflectance data in the blue, green, red, near-infrared and shortwave infrared, to calculate the fractions of soil, vegetation and shade endmembers within the pixel. For BA detection, however, most studies focus exclusively on the information provided by the shade fraction. In this fraction, not only BA but also other targets with similar spectral response may be enhanced, e.g. cloud shadow and water [10]. Therefore, for separation of BA from other targets there is the need of applying a filtering on the shade fraction image to eliminate the confounding features [3].

Although the LSMM presents high accuracy, the procedure for achieving the final burned area map is not yet fully automated, which may be a problem considering the need for processing the currently massive data volume [4, 7, 8].

An alternative to the application of the LSMM on medium spatial resolution data is the use of Spectral Indices (SI), which enhance some useful information through the algebraic combination of spectral bands. These SI are widely used and already consolidated in the literature [11]. The SI has a wide variety of formulations and each index has a better performance according to the user's application [12]. However, SIs are normally generic and do not take into account local features. For instance, SI for BA detection may enhance not only BA but also shadows and water targets. For this reason, the use of SI often requires a filtering step.

Considering that there is a lack of methods for automatically detect BA using medium resolution satellite images in the Brazilian Amazonia, we aimed in this study to present a test-case based on the combination of 10 SI in remote sensing images with three channels composition (Red; Green; Blue - RGB) in order to highlight burned areas from other targets such as vegetation and water. This process generated 120 possible combinations without repetition for medium spatial resolution data. The five most inaccurate and accurate indices were analyzed.

2. SIC-BA: SPECTRAL INDICES COMBINATION FOR BURNED AREA DETECTION

This test-case was performed in a Landsat-8/OLI scene (path/row 221/064, date: 08/17/2014), with 30m of spatial resolution. The study area represents the transition zone between the Amazonia and the Brazilian Savanna (Cerrado) in the Maranhão state.

First, we selected 10 burn, vegetation and water indices (Table 1) and we normalized all indices between [-1;+1]. Aiming to highlight BA from other targets, burn indices were converted to positive values, while vegetation and water indices were converted to negative values. In such a way, BA was visually brighter than other targets in RGB composition.

The SI combination process was performed using a simple three channels (RGB) remote sensing image composition, and generated 120 possible combinations. The order of the SI in the composition was not relevant, therefore, the same indices in different combinations were not considered. After the generation of the 120 RBG compositions, we classified and filtered the results (Subsection 2.1.). Next, we assessed their accuracy according to a reference map, which was performed by a high skilled expert, as proposed by [7] (Subsection 2.2.). Finally, we analyzed the most accurate SIC-BA aiming to identify possible rules and patterns.

2.1. Classification and Filtering Process

The clustering process was performed through the unsupervised algorithm K-means (K=8), according to empirical analysis, followed by a classification step. The two filtering processes were: (i) mode, and (ii) cloud shadow and water filtering. Mode filter was applied, with a windows size of 3, considering the necessity to remove noise along the image. Filtering cloud shadow and water was required due to its similar spectral response with BA [4] through *Fmask* algorithm [13], [14].

It is also important to highlight that all the data processing of this study was executed on a computer with Intel Core i7-2600 processor and 16 GB RAM in Python programming language. It took about 60 hours to process the data, which corresponds a total of 2.5 days of non-stopping data processing.

2.2. Accuracy Assessment

The accuracy assessment performed through a Cohen's Kappa coefficient [25] and a reference map comparison. This mapping was generated through filtering and manual edition steps on a shade fraction from LSMM by means of K-means (K=7), defined through empirical analysis. This phase was performed by a high skilled expert, as proposed by [7].

3. SIC-BA ANALYSIS

The application of the 120 RBG compositions in the study area resulted in a kappa ranging from 0.21 to 0.86, R:NBR2/G:SAVI/B:EVI (Table 2) and R:BAI/G:SR/B:NDVI, respectively (Table 3). The compositions with the lowest accuracy included mainly MIRBI, NBR2, EVI, MNDWI and CSI indices, which may indicate that blue (0.45 - 0.51 μm) and green (0.53 - 0.59 μm) reflectance band are not relevant for BA detection.

Kappa coefficients of the 5 most accurate compositions in study area were relatively high, between 0.85 and 0.86. This composition was R:BAI/G:SR/B:NDVI (Figure 1). Besides that, the most decisive indices were BAI and NDVI, with red (0.64 - 0.67 μm) and near-infrared (0.85 - 0.88 μm) bands, indicating the importance of such indices and bands for BA detection. Finally, SR was identified in both groups of indices, the most inaccurate and accurate indices, and no final conclusion was possible for this index.

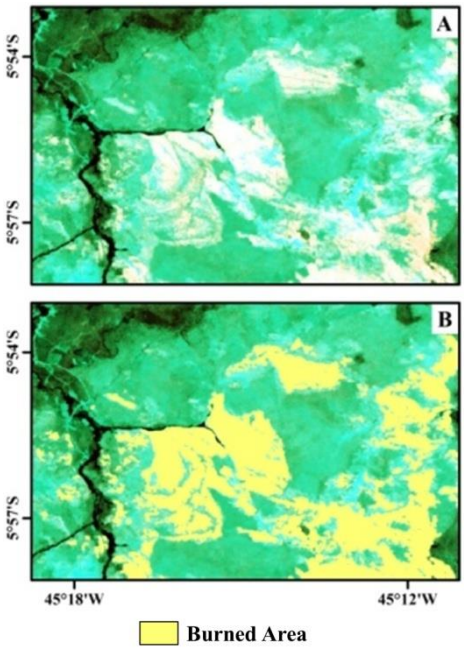

Figure 1. Most accurate SIC-BA in the study area (BAI/SR/NDVI). (A) Subset of study area 1, where white regions represent burned areas. (B) Fig. 2A + BA according to the reference map.

4. CONCLUSIONS

The SI combination was developed considering the different targets that spectral indices may enhance. For BA, the combination accuracy ranged from 0.21 to 0.86 and the most suitable combinations included the indices BAI and NDVI. Neither the vegetation indices SAVI and EVI nor the water index MNDWI were important

Table 1. Spectral indices used in the test-case structure.

Spectral Indices	Initials	Formula	References	Index Type
Simple Ratio	SR	$\frac{\rho NIR}{\rho Red}$	[15]	Vegetation
Normalized Difference Vegetation Index	NDVI	$\frac{\rho NIR - \rho Red}{\rho NIR + \rho Red}$	[16]	Vegetation
Soil Adjusted Vegetation Index	SAVI	$\frac{(1+L)(\rho NIR - \rho Red)}{(\rho NIR + \rho Red + L)}$	[17]	Vegetation
Mid-Infrared Burn Index	MIRBI	$10\,\rho LSWIR - 9.8\,\rho SWIR + 2$	[18]	Burned
Enhanced Vegetation Index	EVI	$\frac{G(\rho NIR - \rho Red)}{(L + \rho NIR + C_1\rho Red - C_2\rho B)}$	[19]	Vegetation
Burned Area Index	BAI	$\frac{1}{(0.1 - \rho Red)^2 + (0.06 - \rho NIR)}$	[20]	Burned
Normalized Burn Ratio	NBR	$\frac{\rho NIR - \rho SWIR}{\rho NIR + \rho SWIR}$	[21]	Burned
Normalized Burn Ratio 2	NBR2	$\frac{\rho SWIR - \rho LSWIR}{\rho SWIR + \rho LSWIR}$	[22]	Burned
Modified Normalized Difference Water Index	MNDWI	$\frac{\rho G - \rho SWIR}{\rho G + \rho SWIR}$	[23]	Water
Char Soil Index	CSI	$\frac{\rho NIR}{\rho LSWIR}$	[24]	Burned

ρB = blue reflectance band; ρG = green reflectance band; ρRed = red reflectance band; ρNIR = near-infrared reflectance band; ρSWIR = short wavelength infrared band; ρLSWIR = long short wavelength infrared band ; L (SAVI) = constant value of soil adjustment (0.5); L (EVI) = constant value (1.0); G = constant value (2.5); C1 = constant value (6.0); C2 = constant value (7.5)

Table 2. Comparison of most inaccurate compositions in the study area.

Compositions			Kappa Coefficient
MIRBI	NBR2	EVI	0.46
NBR2	SR	CSI	0.45
MIRBI	NBR2	SR	0.37
NBR2	EVI	CSI	0.27
NBR2	SAVI	EVI	0.21

Table 3. Comparison of most accurate compositions in the study area.

Compositions			Kappa Coefficient
BAI	SR	NDVI	0.86
BAI	NDVI	CSI	0.86
NBR	BAI	SR	0.86
NBR	BAI	CSI	0.85
NBR	BAI	NDVI	0.85

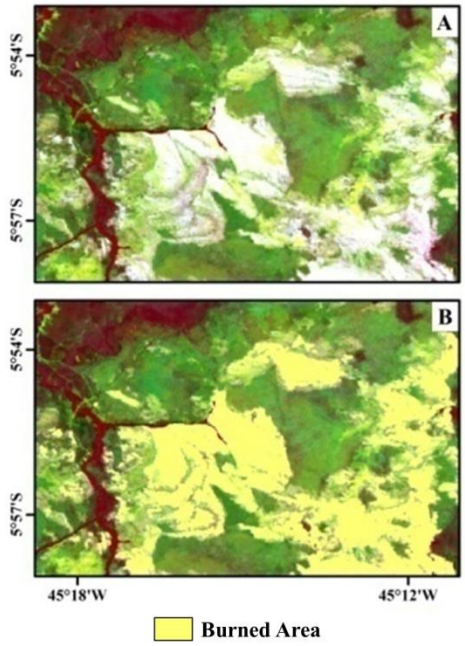

Figure 2. Most accurate SIC-BA in the study area 2 (MIRBI/NBR/BAI). (A) Subset of study area 1, where white regions represent burned areas. (B) Fig. 3A + BA according to the reference map.

for BA detection in study area. In such a way, we indicate as future researches a new round of test-case with the substitution of them to others BA indices.

Furthermore, it is important to highlight that due to Amazonia heterogeneity, it is necessary to analyze the performance of the most impressive combinations in others areas, such as for consolidated agriculture and pasture regions, in order to identify the most indication combination of SI for BA detection in Brazilian Amazonia.

5. ACKNOWLEDGMENT

We would like to thank the National Council for Scientific and Technological Development (CNPq), processes 131241/2016-8, 140377/2018-2, 309247/2016-0 and 16/02018-2, the Coordination for the Improvement of Higher Education Personnel (CAPES), code 001, and the grant #2017/24086-2, São Paulo Research Foundation (FAPESP), for the research financial support.

6. REFERENCES

[1] L. E. O. C. Aragão, L. O. Anderson, M. G. Fonseca, T. M. Rosan, L. B. Vedovato, F. H. Wagner, C. V. J. Silva, C. H. L. Silva Junior, E. Arai, A. P. Aguiar, J. Barlow, E. Berenguer, M. N. Deeter, L. G. Domingues, L. Gatti, M. Gloor, Y. Malhi, J. A. Marengo, J. B. Miller, O. L. Phillips, and S. Saatchi, "21st Century drought-related fires counteract the decline of Amazon deforestation carbon emissions," *Nat. Commun.*, vol. 9, no. 1, 2018.

[2] L. E. O. . Aragao, Y. Malhi, N. Barbier, A. Lima, Y. Shimabukuro, L. Anderson, and S. Saatchi, "Interactions between rainfall, deforestation and fires during recent years in the Brazilian Amazonia," *Philos. Trans. R. Soc. B Biol. Sci.*, vol. 363, no. 1498, pp. 1779–1785, 2008.

[3] Y. E. Shimabukuro, J. Miettinen, R. Beuchle, R. C. Grecchi, D. Simonetti, and F. Achard, "Estimating Burned Area in Mato Grosso, Brazil, Using an Object-Based Classification Method on a Systematic Sample of Medium Resolution Satellite Images," *IEEE J. Sel. Top. Appl. Earth Obs. Remote Sens.*, vol. 8, no. 9, pp. 4502–4508, 2015.

[4] L. O. Anderson, D. Cheek, L. E. Aragao, L. Andere, B. Duarte, N. Salazar, A. Lima, V. Duarte, and E. Arai, "Development of a Point-based Method for Map Validation and Confidence Interval Estimation: A Case Study of Burned Areas in Amazonia," *J. Remote Sens. GIS*, vol. 06, no. 01, pp. 1–9, 2017.

[5] L. Giglio, C. Justice, L. Boschetti, and D. Roy, "MCD64A1 MODIS/Terra+Aqua Burned Area Monthly L3 Global 500m SIN Grid V006 [Data set]," *NASA EOSDIS L. Process. DAAC*, 2015.

[6] M. Ehlers, R. Janowsky, and M. Gaehler, "New remote sensing concepts for environmental monitoring," *Remote Sens. Environ. Monit.*, vol. 4545, pp. 1–12, 2002.

[7] L. O. Anderson, L. E. O. E. C. De Aragão, A. De Lima, and Y. E. Shimabukuro, "Detecção de cicatrizes de áreas queimadas baseada no modelo linear de mistura espectral e imagens índice de vegetação utilizando dados multitemporais do sensor MODIS/TERRA no estado do Mato Grosso, Amazônia brasileira," *Acta Amaz.*, vol. 35, no. 4, pp. 445–456, 2005.

[8] A. Lima, T. S. F. Silva, L. E. O. e C. de Aragão, R. M. de Feitas, M. Adami, A. R. Formaggio, and Y. E. Shimabukuro, "Land use and land cover changes determine the spatial relationship between fire and deforestation in the Brazilian Amazon," *Appl. Geogr.*, vol. 34, pp. 239–246, 2012.

[9] Y. E. Shimabukuro and J. A. Smith, "The Least-Squares Mixing Models to Generate Fraction Images Derived From Remote Sensing Multispectral Data," *IEEE Trans. Geosci. Remote Sens.*, vol. 29, no. 1, pp. 16–20, 1991.

[10] E. Chuvieco and R. G. Congalton, "Mapping and inventory of forest fires from digital processing of tm data," *Geocarto Int.*, vol. 3, no. 4, pp. 41–53, 1988.

[11] S. Liang, *Quantitative Remote Sensing of Land Surfaces*. Hoboken, NJ, USA: John Wiley & Sons, Inc., 2003.

[12] A. R. Formaggio and I. D. Sanches, *Sensoriamento remoto em agricultura*, 1st ed. São Paulo: Oficina de textos, 2017.

[13] Z. Zhu and C. E. Woodcock, "Object-based cloud and cloud shadow detection in Landsat imagery," *Remote Sens. Environ.*, vol. 118, pp. 83–94, Mar. 2012.

[14] Z. Zhu, S. Wang, and C. E. Woodcock, "Improvement and expansion of the Fmask algorithm: cloud, cloud shadow, and snow detection for Landsats 4–7, 8, and Sentinel 2 images," *Remote Sens. Environ.*, vol. 159, pp. 269–277, Mar. 2015.

[15] G. S. Birth and G. R. McVey, "Measuring the Color of Growing Turf with a Reflectance Spectrophotometer1," *Agron. J.*, vol. 60, no. 6, p. 640, 1968.

[16] J. W. J. Rouse, R. H. Haas, J. A. Schell, and D. W. Deering, "Monitoring vegetation systems in the Great Plains with ERTS," in *Third ERTS Symposium*, 1974, pp. 309–317.

[17] A. . Huete, "A soil-adjusted vegetation index (SAVI)," *Remote Sens. Environ.*, vol. 25, no. 3, pp. 295–309, Aug. 1988.

[18] S. Trigg and S. Flasse, "An evaluation of diVerent bi-spectral spaces for discriminating burned shrub-savannah," *Int. J. Remote Sens.*, vol. 22, no. 13, pp. 2641–2647, 2001.

[19] A. Huete, K. Didan, T. Miura, E. P. Rodriguez, X. Gao, and L. G. Ferreira, "Overview of the radiometric and biophysical performance of the MODIS vegetation indices," *Remote Sens. Environ.*, vol. 83, no. 1–2, pp. 195–213, 2002.

[20] E. Chuvieco, M. P. Martín, and A. Palacios, "Assessment of different spectral indices in the red-near-infrared spectral domain for burned land discrimination," *Int. J. Remote Sens.*, vol. 23, no. 23, pp. 5103–5110, 2002.

[21] C. H. Key and N. C. Benson, "Landscape Assessment: Ground measure of severity, the Composite Burn Index; and Remote sensing of severity, the Normalized Burn Ratio," Ogden, UT, 2006.

[22] E. Vermote, C. Justice, M. Claverie, and B. Franch, "Preliminary analysis of the performance of the Landsat 8/OLI land surface reflectance product," *Remote Sens. Environ.*, vol. 185, pp. 46–56, Nov. 2016.

[23] H. Xu, "Modification of normalised difference water index (NDWI) to enhance open water features in remotely sensed imagery," *Int. J. Remote Sens.*, vol. 27, no. 14, pp. 3025–3033, Jul. 2006.

[24] A. M. S. Smith, N. A. Drake, M. J. Wooster, A. T. Hudak, Z. A. Holden, and C. J. Gibbons, "Production of Landsat ETM+ reference imagery of burned areas within Southern African savannahs: Comparison of methods and application to MODIS," *Int. J. Remote Sens.*, vol. 28, no. 12, pp. 2753–2775, 2007.

[25] K. Congalton, R. G., & Green, *Assessing the accuracy of remotely sensed data. Principles and practices (2 edition)*. 2009.